Full paper

# Non-contact and liquid–liquid interfacing triboelectric nanogenerator for self-powered water/liquid level sensing

Peng Wang [a,b,c], Steven Zhang [a], Lei Zhang [a], Longfei Wang [a], Hao Xue [a], Zhong Lin Wang [a,d,*]

[a] School of Materials Science and Engineering, Georgia Institute of Technology, Atlanta, GA, 30332-0245, USA
[b] Key Lab of Marine Environmental Corrosion and Biofouling, Institute of Oceanology, Chinese Academy of Sciences, Qingdao, 266071, China
[c] Center for Ocean Mega-Science, Chinese Academy of Sciences, 7 Nanhai Road, Qingdao, 266071, China
[d] Beijing Institute of Nanoenergy and Nanosystems, Chinese Academy of Sciences, Beijing, 100049, China

ABSTRACT

Triboelectric nanogenerators (TENG) based on liquid-solid or solid-solid contact have attracted much attention in sensing applications recently. However, the stain caused from external environment and high friction over triboelectric interface are two important issues yet to be solved. To address these issues, a novel magnetic field assisted non-contact TENG is designed by driving the motion of ferrofluid in a sealed tube under an external magnetic field without direct contact. The as-designed TENG can separate the external mechanical motion from the inner triboelectric process, thereby solving the potential stain problem over the triboelectric interface from external environment. Furthermore, a lubricant oil layer is introduced between ferrofluid and substrate to construct a liquid–liquid triboelectric interface, which facilitates the sliding behavior of ferrofluid. This design helps to extend the range of linear relationship between triboelectric current peak value and the ferrofluid motion velocity over its surface, thereby breaking the motion velocity measurement limit of TENG as a velocity sensor. Finally, its potential application is demonstrated as a self-powered water/liquid level sensor. This work provides a novel type of non-contact TENG, and shows triboelectrification on liquid–liquid contact. The novel TENG could be further applied as a highly sensitive sensor in harsh environment.

## 1. Introduction

Triboelectric nanogenerators (TENG) have attracted much attention for their applications in self-powered active sensing [1–8]. Recently, they have been demonstrated to be effective as tactile and rotation sensors based on solid/solid contact [9–14], and as wave, acceleration, and liquid sensors based on liquid/solid contact [14–20]. However, there are still some issues that need to be addressed for their self-powered sensing applications.

Firstly, the triboelectric layer can easily be stained by biofouling and chemical stains from the external environment during TENG's practical application [21,22]. The stain over interface would thus affect the output of TENG, thereby bringing a deviation to the TENG sensor. This problem could be solved by designing a non-contact TENG that can separate the triboelectric charging interface with the external environment [23–25]. Ferrofluid is a kind of material that could be actuated by an applied external magnetic field [26–28]. By applying a magnetic field, the ferrofluid, which is placed inside a closed container that is

separated from the external environment, would move along the flow. Owing to the triboelectric effect at liquid-liquid interface, the ferrofluid's motion is converted into an electric signal. Thus, with the ferrofluid, the TENG is separated from the external environment, which would prevent the triboelectric layer to be stained, whether from biofouling, or chemical stain from the external environment. The introduction of ferrofluid brings new opportunity for the design of novel non-contact TENG, and further extends the applications of non-contact TENG. To the best of our knowledge, this is the first report about design of non-contact TENG based on ferrofluid.

Secondly, sensitivity, but not high electric output, is the most important parameter for the design of self-powered triboelectric sensor. High friction always exists in the traditional solid/solid and solid/liquid contact sliding and freestanding triboelectric models, which are not the best choices for the sensor design in practical applications. For example, in liquid-solid contact, friction exists on the interface results in a relative motion velocity limit between each other. In a case that water flows with a velocity exceeding the limit, the friction would result in a deformation

of water flow, which would cause a water droplet or a thin water-based film to be left behind. Consequently, the signal generated by liquid-solid interfacing TENG sensor could not reflect the real water motion. Recently, liquid-liquid interfacing triboelectric process has been demonstrated [29,30]. It could be utilized to improving the test accuracy of TENG sensor for its advantage in reducing friction on the triboelectric interface of TENG, but it still requires experiment verification.

Here, in this work, a novel magnetic field assisted non-contact and liquid–liquid interfacing TENG (LLi-TENG) was proposed to solve the above-mentioned problems of traditionally designed TENG in self-powered sensing application. To realize the non-contact behavior, ferrofluid was injected into a sealed polytetrafluoroethylene (PTFE) tube wrapped with grounded copper (Cu) electrodes on the exterior of the tube. The ferrofluid's sliding behavior in the tube is caused by an external magnet ring, and the ferrofluid's motion would induce electron transfer between Cu electrode and ground. To construct a liquid-liquid triboelectric interface, lubricant oil perfluoropolyethers (PFPE) was introduced between ferrofluid/PTFE tube interface, and it facilitates the ferrofluid sliding behavior over its surface. The working principle of the LLi-TENG was proposed based on finite-element simulations and verified with experimental results. To prove its potential applications as a motion velocity sensor and a location detector, the relationship between external magnet's motion velocity and the TENG short-circuit current peak value was investigated, and characteristics peak positions of both open-circuit potential and short-circuit current were analyzed to correspond with the location of external magnet ring. The linear relationship range of LLi-TENG was compared with that of liquid-solid interfacing TENG to demonstrate the advantage of introducing lubricant oil layer into triboelectric interface, and the results were explained based on the surface roughness analysis. Finally, the potential application of the non-contact LLi-TENG was demonstrated by its use as a water level sensor, and its advanced performance was proven in simulated polluted water environment. This research extends the possible application area of TENG, especially as a self-powered and highly sensitive sensor in harsh environment.

## 2. Material and methods

### 2.1. Fabrication of TENG

Two kinds of polytetrafluoroethylene (PTFE) tubes with length of 18 cm were utilized for the fabrication of LLi-TENG, which are the inner tube with inner diameter of 1.270 cm and thickness of 0.159 cm, and the outer tube with inner diameter of 1.905 cm and thickness of 0.159 cm, respectively. A certain volume of lubricant oil perfluoropolyethers was dropped over the inner surface of inner tube, and then spread it over the inner tube surface using a PTFE film with contact area of 0.3 cm$^2$, which is much less than the total surface area of tube surface (around 71.8 cm$^2$). After being spread over the entire tube surface, the lubricant layer was then left to stand in ambient condition for 2 h, to let it further spread over under gravity and surface tension. The thickness of lubricant (CA. 1 μm–50 μm) can be controlled by the volume of lubricant dropped. 0.2 mL commercial water-based ferrofluid EMG 607 (Ferrotec, Corp., Santa Clara, CA, USA) was dropped into the inner tube. Copper tape with width of 0.6 cm was wrapped over outer surface of the inner tube as ring electrodes. The inner tube was then covered with insulation polymer and copper tape, and inserted into the outer PTFE tube. The two tubes were then sealed with water-proof tape. To prove the advantage of liquid-liquid interfacing triboelectric model in improving the LLi-TENG performance as a sensor, a similar liquid-solid interfacing TENG (LSi-TENG) was fabricated with the sample procedure except that there is no lubricant oil between ferrofluid/PTFE tube interface.

To design a water level sensor, a ferromagnetic ring covered with hollow acrylic was utilized for reflecting the water level. The air in the acrylic helps to increase the buoyancy to magnet, thereby making the

magnet ring floating over water level.

### 2.2. Electrical measurement and surface analysis

The open-circuit voltage and short-circuit current were measured by using a Keithley 6514 system electrometer. The morphology of slippery lubricant PFPE-infused layer was characterized by an atomic force microscopy (AFM).

### 2.3. Simulation model for the LLi-TENG

The proposed model is based on a ferrofluid layer with thinkness of 1 mm, and 6 mm wide Cu electrode wrapped on a PTFE tube with inside diameter of 1.270 cm and thickness of 0.159 cm. The triboelectric charge density on the surfaces of the ferrofluid and lubricant oil over PTFE tube is assumed to be 1 μC m$^{-2}$.

## 3. Results and discussion

Fig. 1 shows the schematic of LLi-TENG. As shown in Fig. 1a, a lubricant PFPE-infused layer was fabricated over the inner surface of inner PTFE tube. Copper ring electrodes over outer surface of inner tube were connected with ground, and the distance between each ring electrodes was controlled according to experiment need. The inner surface of outer tube was entirely covered with copper electrode, which was utilized for blocking the external effect to the signal by connecting with the ground. An insulating polymer was inserted between inner tube and outer tube to avoid contact between the electrodes. The magnet ring out of tube can drive the synchronized motion of ferrofluid with external mechanical motion under magnetic field. A PTFE tube was selected as outer tube, because the PTFE is a kind of material with good anti-fouling performance, thereby solving the problem that the friction resistance between tube and external magnetic ring increases for the biofouling in practical application. The detailed fabrication process is described in the Experimental Section. The fabricated TENG is apparently composed of as-designed nested tubes and a magnet ring covered with acrylic, and its photo is shown in Fig. 1b.

To illustrate the effect of lubricant oil on the relative motion of the ferrofluid, contact angle measurements were performed. The contact angle of ferrofluid on PTFE is 103.5 ± 3° (Fig. 1c1) for the inherent hydrophobic property of PTFE. In contrast with that, the contact angle of lubricant PFPE on PTFE is lower than 10° (Fig. 1c2). Since the PTFE presents a better chemical affinity to lubricant oil than the ferrofluid [28–30], the lubricant oil over PTFE can be hardly replaced by ferrofluid, which is evidenced by the fact that the ferrofluid droplet steadily stands over slippery lubricant oil-infused surface (Fig. 1c3). Under applied magnetic field, the ferrofluid droplet spreads over slippery lubricant oil-infused PTFE surface and presents in a form of thin layer (Fig. 1c4). The sliding contact angles of ferrofluid droplet were measured on both bare PTFE and slippery lubricant oil-infused surface. It is clear that the ferrofluid droplet still sticks over bare PTFE surface with a titled angle of 25° (Fig. 1c5). In contrast, the droplet can easily slide off slippery lubricant oil-infused layer with a titled angle of around 5° (Fig. 1c6), indicating that slippery lubricant oil-infused layer would facilitate the sliding of ferrofluid for its low attraction between PFPE and ferrofluid. The easier sliding behavior of water-based ferrofluid over lubricant oil-infused layer can be attributed to the insolubility between lubricant oil PFPE and ferrofluid, and also the low roughness of slippery lubricant oil-infused layer evidence by AFM (Figs. S1 and S2). This provides the primary advantage for constructing the liquid/liquid contact triboelectric model, as the liquid/liquid contact allows easier motion of the ferrofluid. It should be noticed that the ferrofluid droplet slides off the slippery lubricant oil-infused layer with a constant velocity (Fig. 1c6), indicating the lubricant oil can completely cover the substrate after the fabrication procedure.

Fig. 2a illustrates the working principle of LLi-TENG under short-
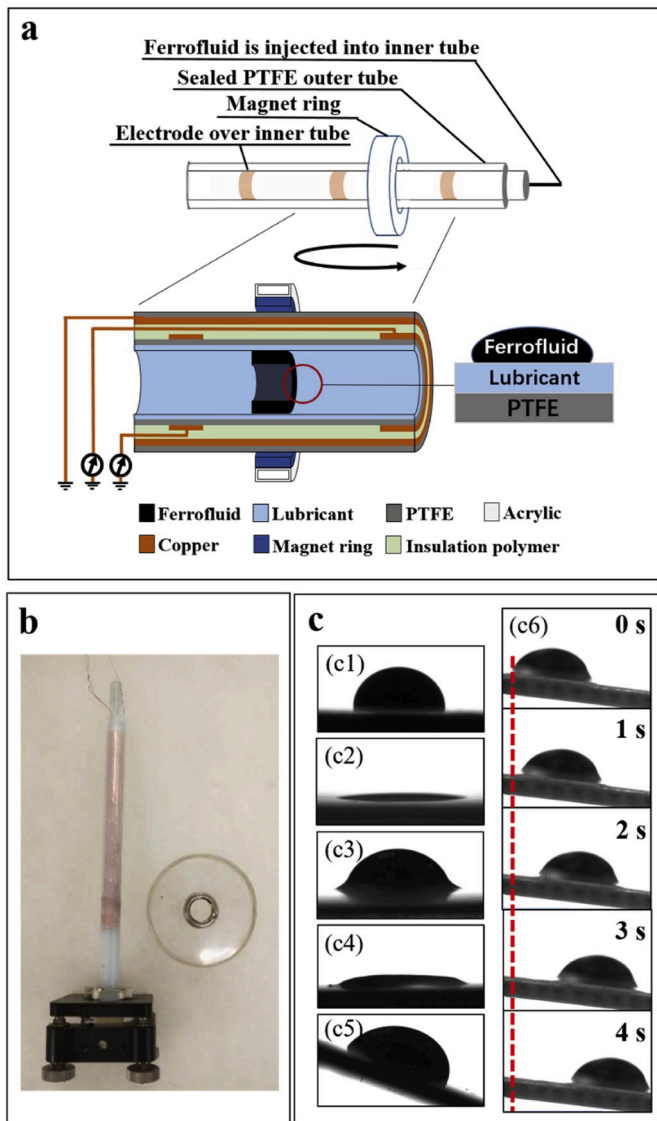
**Fig. 1.** The schematic for the non-contact LLi-TENG and the related wettability characterization. (a) The schematic of magnetic field assisted non-contact LLi-TENG; (b) The photograph of the magnetic field assisted non-contact LLi-TENG; (c) The photographs of droplets on samples: (c1) ferrofluid droplet on PTFE, (c2) lubricant oil PFPE droplet on PTFE, (c3) ferrofluid droplet on lubricant oil-infused PTFE surface, (c4) ferrofluid droplet on lubricant oil-infused PTFE surface under action of underneath magnetic field, (c5) ferrofluid droplet on titled PTFE with angle of 25°, (c6) dynamic action of ferrofluid droplet on lubricant oil-infused PTFE surface with titled angle of 5°.

circuit condition. The water-based ferrofluid was fabricated by dispersing magnetic $Fe_3O_4$ nanoparticles into water with the assistance of surfactant. It is believed that the $Fe_3O_4$ nanoparticles are covered with water molecules. Thus, the triboelectric charging behavior of LLi-TENG actually occurs on the water/lubricant oil interface. For the existence of high surface electron affinity atoms, Fluorine and Oxygen atoms, in the chemical structure of lubricant oil PFPE, it most likely to attract electrons from the water, causing a net negative charges in lubricant oil PFPE and a net positive charges in the ferrofluid. The generated negative triboelectric charges distribute evenly over the slippery lubricant oil-infused surface, and they can remain for a period of time for the insulation property of lubricant oil PFPE. At the original position (Fig. 2a-i), these negative triboelectric charges remain over lubricant oil-infused surface would induce some electrons flow from the Cu electrode to the ground. Once the ferrofluid droplet approaches the Cu electrode, its

positive triboelectric charges will drive electrons to flow from the ground to the Cu electrode, as shown in Fig. 2a-ii. The electrons continue to flow to the Cu electrode until the center of ferrofluid droplet is aligned with the center of electrode (Fig. 2a-iii). With the ferrofluid droplet slides away from the Cu electrode, the induced electrons flow back to the ground (Fig. 2a-iv), and finally the device returns to its original state (Fig. 2a-v) as the ferrofluid is far from the electrode. Consequently, an alternating current signal would be generated with the ferrofluid droplet approaching and leaving the electrode, and it can be utilized as an indicator for the position of ferrofluid droplet.

The COMSOL Multiphysics software based on finite-element simulation is employed to calculate the potential distribution of three typical states under open-circuit condition, as shown in Fig. 2b. The calculated potential distribution across the electrode is consistent with the proposed working principles. With the ferrofluid droplet sliding from left to the middle position (the upper position of electrode), the potential on electrode gets more positive (Fig. 2b-i, 2b-ii, 2b-iii), inducing the electron flow from the ground to the copper electrode. After the ferrofluid droplet slides away from electrode (Fig. 2b-iv, 2b-v), the potential on electrode gets more negative, and it induces the electrons transferring from electrode to the ground.

The working process of LLi-TENG with only one copper electrode was investigated under various external magnet motion velocity driven by linear motor. Fig. 3a presents the short-circuit current of the LLi-TENG with PFPE lubricant oil layer thickness of 50 μm working under different external magnet motion velocity ranging from 0.02 cm/s to 15 cm/s. Within the velocity range from 0.02 cm/s to 5 cm/s, the short-circuit current peak value of TENG increases with the motion velocity, while the peak value of open circuit potential maintains at around 1.3V and is independent of motion velocity (Fig. S3). However, short-circuit current peak value does not increase proportionally with the velocity in case that the velocity increases up to 10 cm/s, and it even decreases if the velocity further increases to 15 cm/s. Based on these primary data, it is clear that there exists a linear relationship between short-circuit current peak value of LLi-TENG under the motion velocity ranging from 0.02 cm/s to 5 cm/s (Fig. 3b), indicating that LLi-TENG current signal can be utilized for detecting the motion velocity within this range. However, the short-circuit current peak value would be out of the linear relationship in case that the motion velocity is higher than 5 cm/s. This can be attributed to the fact that the ferrofluid droplet gets deformed if its motion velocity is greater than the limited value (Fig. 3e). The deformation of ferrofluid droplet would increase its contact area with lubricant oil-infused surface and reduce the charge density on the ferrofluid/lubricant contact interface. Consequently, the inducted electron over the copper electrode with a constant area would be reduced, and the short-circuit current peak value got decreased. As a comparison, a LSi-TENG was fabricated with the same procedure of LLi-TENG except that there is no lubricant oil over the inner surface of inner tube. Similar with LLi-TENG, the short-circuit current peak value of LSi-TENG increases with the motion velocity within the range between 0.02 cm/s and 1 cm/s, and decreases in case that the velocity increases up to 5 cm/s (Fig. 3c). However, a linear relationship between short-circuit current and motion velocity only exists in the range from 0.02 cm/s to 0.1 cm/s (Fig. 3d), which is more than one order of magnitude narrower than that of the LLi-TENG. This is attributed to the fact that bare PTFE presents higher attraction to ferrofluid ($f_2$) than slippery lubricant oil-infused surface ($f_1$), thereby decreasing the limited value of ferrofluid motion velocity. This is evidenced by the phenomenon that the ferrofluid droplet gets deformed and even leaves a visible water layer over PTFE (shown in the red circled area of Fig. 3e), in case that it slides with a motion velocity even down to 1 cm/s. It can be expected that the lubricant oil layer that was introduced between ferrofluid and substrate facilitates the sliding behavior of ferrofluid, due to the insoluble property between water and lubricant oil [31,32][33], and also due to the low roughness of lubricant oil layer from the figures taken by AFM (Figs. S1 and S2).
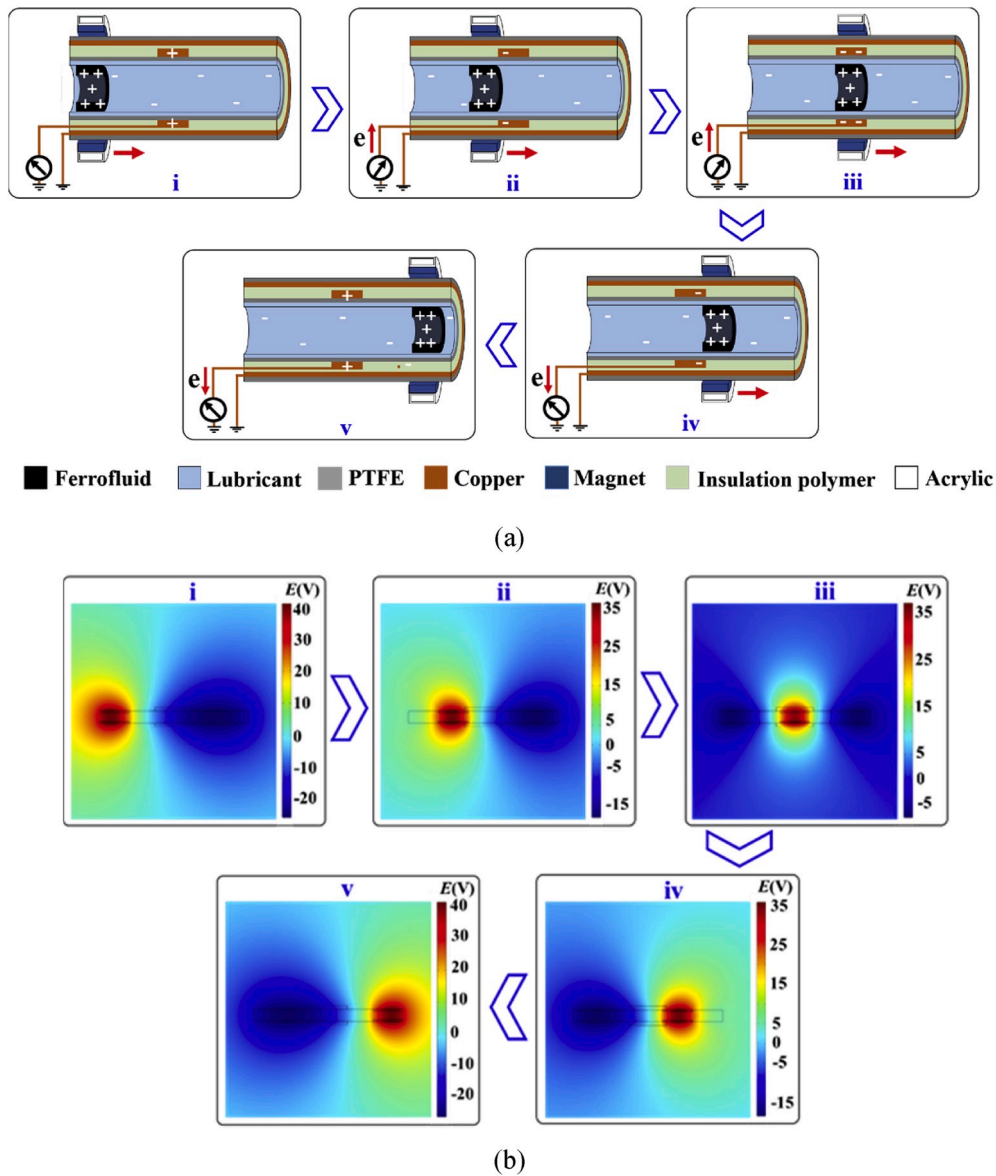
Fig. 2. The working principle of LLi-TENG (a) and the simulation results (b).

We investigated the effect of lubricant oil layer thickness to the short-circuit current of LLi-TENG. As we expected, the thicker lubricant oil layer results in the decrease of circuit current peak value. It can be attributed to the fact that the thick lubricant oil layer would reduce the induction of electrons on the electrode from the ferrofluid. Regarding to all the LLi-TENG with lubricant oil layer thickness ranging from 1 μm to 20 μm, the short-circuit current peak value of TENG increases with the motion velocity (Fig. S4), similar with the result of the LLi-TENG with lubricant oil layer of 50 μm. There is also a linear relationship between short circuit current peak value and motion velocity for each LLi-TENG, and the slope value increases with the decrease of lubricant oil layer thickness (Fig. 3f). The linear relationship between velocity and short-circuit current for low thickness lubricant (1 μm–20 μm) only occurs at velocities from 0.02 cm/s to 1 cm/s, which is narrower than that of TENG with lubricant oil layer of 50 μm. It is indicated that the thinner lubricant oil layer would result in the narrowing of linear relation between short circuit current peak value and motion velocity, which might be attributed to the increase of friction between lubricant oil-infused surface and ferrofluid for the decrease of lubricant oil. In our opinion, many factors would affect the slope value of short circuit current peak value/motion velocity relationship for each LLi-TENG. For example, the

short circuit current peak value of the LLi-TENG would be related to the electrode area, which is affected by the tube diameter, wideness of electrode, and so forth. Thus, the slope value of the linear relationship should be tested and corrected for each LLi-TENG before it was utilized as water level sensor. In addition to the potential application in detecting the instantaneous motion velocity of outer magnet ring over electrode by utilizing the current, the LLi-TENG can sense other motion characteristics of outer magnet (such as location, average velocity between electrodes), if an array of Cu electrodes is fabricated along the inner PTFE tube (Fig. 4). Three Cu electrodes with a width of 6 mm were evenly distributed along the inner PTFE tube with a uniform interval of 9 mm between each other, and were connected in parallel to an electrometer (Fig. 4c). The moving velocity of outer magnet driven by linear motor is set as 1 cm/s, and it drives the motion of ferrofluid droplet in the tube. The electric signals (potential and current) collected were compared with the electric signals collected from each single electrode (Fig. 4a and b). In the case that the three electrodes were connected in parallel to the ground, three potential peaks can be collected when the outer magnet move over tube. Each peak that is measured with three electrodes in parallel appears at the same time point with the signal peak from single electrode when the ferrofluid moves past the ring electrode,
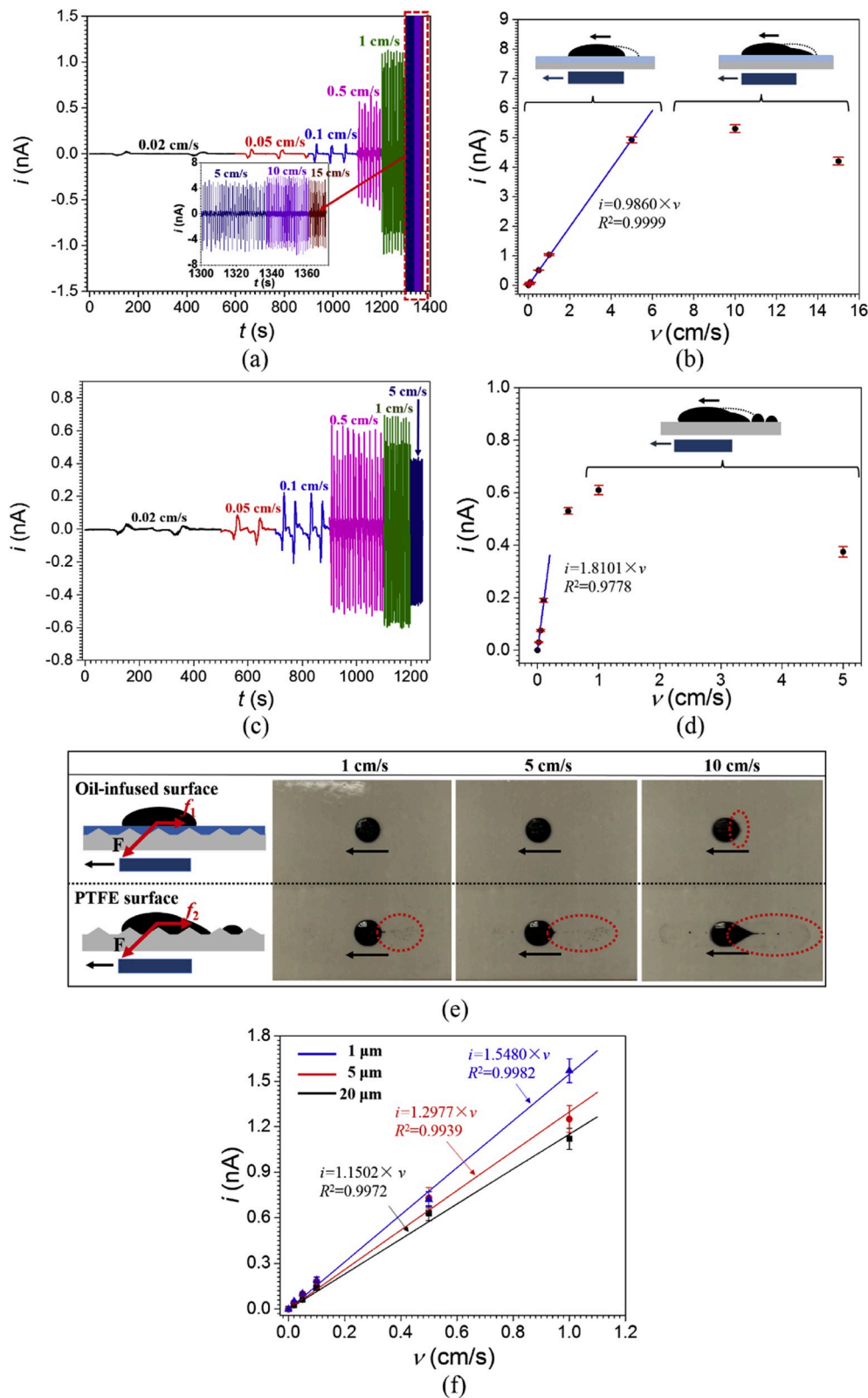
**Fig. 3.** The short-circuit current of LLi-TENG based on slippery lubricant oil-infused surface (a), and the relationship between short-circuit current peak value and moving velocity of ferrofluid driven by magnet (b); The short-circuit current of LSi-TENG based on bare PTFE surface (c), and the relationship between short-circuit current peak value and moving velocity of ferrofluid driven by magnet (d); (e) the ferrofluid droplet photo over slippery lubricant oil-infused surface and bare PTFE surface under different moving velocity ranging from 1 to 10 cm/s, (f) the relationship between short-circuit current peak value of LLi-TENG with different lubricant oil layer thickness (1–20 μm) and moving velocity of ferrofluid driven by magnet.

and they correspond to the location that the ferrofluid droplet center is aligned with the center of each electrode (Fig. 4a). At these three time points. The negative charges reach the maximum value on the Cu electrode, and begin to flow from the electrode to the ground. As a typical electronic signal indicator, the current is changing from negative to positive (Fig. 4b). Both these output signals (open-circuit electric potential and short-circuit current) characteristics can be utilized for identifying the outer magnet location. According to the experimental results, the LLi-TENG can successfully detect the outer magnet location with an accuracy of 15 mm. Actually, the accuracy of LLi-TENG sensor for location determination could be increased by decreasing the wideness of electrodes and the interval between two neighboring electrodes
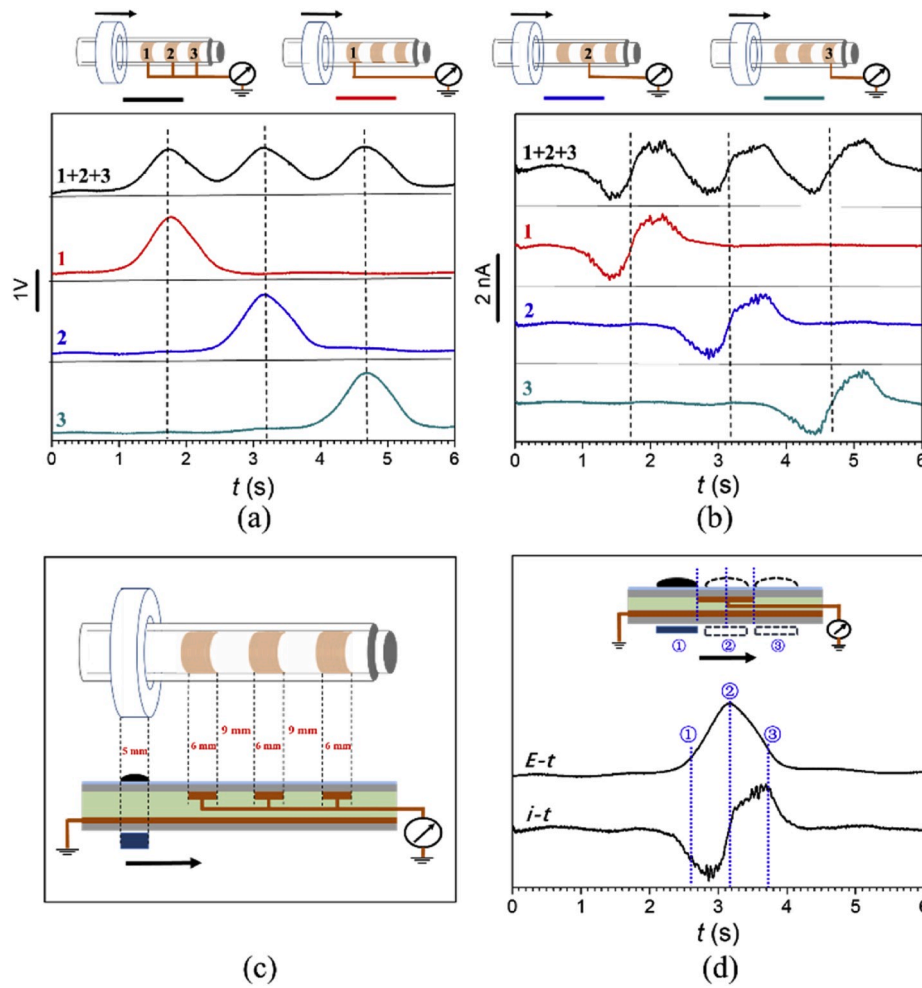
**Fig. 4.** The output performance of non-contact LLi-TENG with ferrofluid motion velocity of 1 cm/s: (a) open-circuit potential, (b) short-circuit current. (c) The schematic showing the dimension of the TENG, (d) the electric signal of TENG corresponding to the typical position of magnet.

in future practical application. The average motion velocity of outer magnet between two electrodes can be calculated by determining the time interval between the characteristic points of electric signal from the two electrodes according the following equation:

$$v = \frac{d}{t} \tag{1}$$

where, $v$ is the average motion velocity of outer magnet between two electrodes, $d$ is the distance between the two electrodes, and $t$ is the time interval between the characteristic points of electric signal. It is clear that the time interval between the characteristic points of electrode 1 and 2 is 1.5 s, which is the same with that between electrodes 2 and 3 (Fig. 4a and b). The average motion velocity can be calculated as 1 cm/s, since the distance between the centers of two electrodes is 15 mm. The calculated average motion velocity is the same as that of the actual one, demonstrating that the electric signal is effective for determining the average motion velocity of outer magnet.

To prove the potential application as a water level sensor, a LLi-TENG demo with lubricant oil layer thickness of 5 μm was immersed into the water in a glass pot with valve, and vertically fixed over a stage. A magnet ring was inserted into hollow acrylic to increase the buoyancy, to make sure that it can float over water level. The LLi-TENG tube was placed inside of the magnet ring, which can drive the flow of ferrofluid in the tube (Fig. 5a). The dimension of the as-fabricated TENG was shown in Fig. 5a, where the width of electrode, the distance between electrodes, and the thickness of magnet ring were labeled. The change of

water level was simulated by allowing water flow out through valve. The motion of magnet ring with water level can drive the motion of ferrofluid in the tube, thereby inducing the electron transfer on electrode. The electric signal generated thus can be utilized to acquire the water level information. We evaluated its performance in both clean water and polluted water with dye and oil (Videos S1 and S2, Fig. 5b). The electric signals of the TENG were monitored in clean water and polluted water with dye and oil under the same water level falling velocity. It can be found that the short-circuit current curves present the same character, and the time spacing between two current peaks are the same. It was proven that the non-contact LLi-TENG can avoid the effect of environment to the electric signal, since it effectively separates the contact of external mechanical motion to the inner triboelectric charging behavior in a sealed room. According to the relationship between motion velocity of magnet and current peak value (Fig. 3f), the water level falling velocity over the electrode can be calculated as 0.137 cm/s based on the current peak value of 0.178 nA (Fig. 5c). It is known that the distance between the centers of two electrodes is 4.30 cm, and the time internal of magnet ring moving over the two electrodes is 30.6 s (Fig. 5c). Thus the decrease velocity of water level can be calculated as 0.141 cm/s. The two values are closed to each other, proving that the TENG sensor can provide accurate water level falling velocity. We also characterized the electric signal of LLi-TENG without injecting ferrofluid into the inner tube (Fig. 5c). No electric signal can be detected, indicating the triboelectric charging behavior between external water and outer PTFE tube would not bring effect the output of TENG for the blocking effect of copper electrode over the inner surface of outer tube. In some special
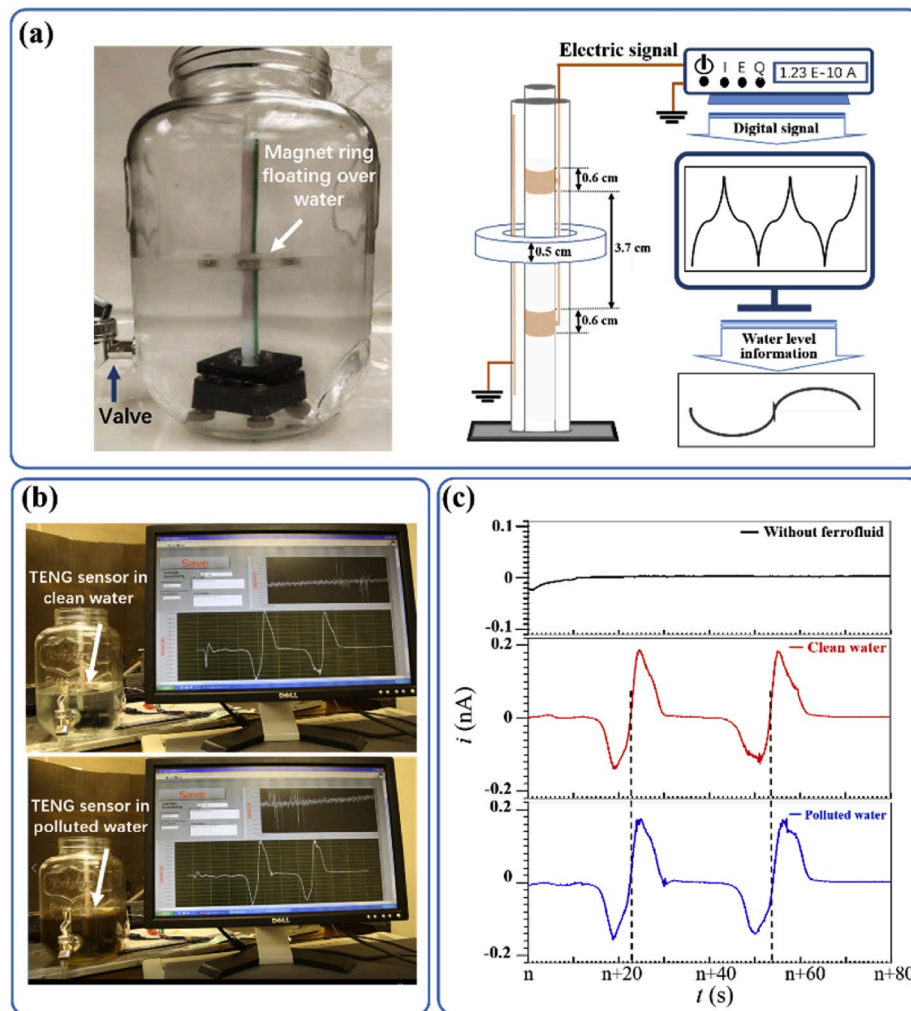
**Fig. 5.** The application of LLi-TENG as a water level sensor. (a) The photograph of LLi-TENG for water level sensor and the schematic of detection process; (b) The detection process of LLi-TENG sensor in clean and polluted water; (c) The electric signal of TENG without ferrofluid, and the LLi-TENGs in clean water and polluted water.

practical application cases, wave fluctuation might affect the electric signals of TENG, such as bringing some unexpected electric signals, thereby affecting the sensing accuracy. We would try to solve this problem by signal processing and analysis in future work.

Supplementary video related to this article can be found at https ://doi.org/10.1016/j.nanoen.2020.104703

## 4. Conclusion

In this work, a novel magnetic field assisted non-contact and liquid-liquid interacting TENG was proposed, and its potential application as a water level sensor was demonstrated. The as-designed non-contact TENG can effectively solve the possible stain problem on the triboelectric interface, by separating the external mechanical motion with the inner ferrofluid triboelectric charging process in a sealed tube. The electric signal generated for the synchronous motion of ferrofluid with the external magnet ring floating over water level can be analyzed to determine the water level position, instant water level motion velocity over electrode, and the average water level motion velocity between two electrodes. Furthermore, the introduction of oil layer between ferrofluid/PTFE interface to construct liquid-liquid contact triboelectric model helps to increase the maximum detection velocity value of external motion from 0.1 cm/s to 5 cm/s, by extending the linear relationship range between triboelectric current peak with external motion velocity. The designed TENG can successfully detect the outer magnet location with an accuracy down to centimeter level. It presents good immune effect to the external condition, even in the polluted water with both dye and oil. This research demonstrated the advantage of non-contact and liquid-liquid interfacing TENG as a self-powered water level sensor. The non-contact TENG would be further applied as a sensor in a harsh environment.

## Declaration of competing interest

We declare that we do not have any commercial or associative interest that represents a conflict of interest in connection with the work submitted.

## CRediT authorship contribution statement

**Peng Wang:** Conceptualization, Methodology, Formal analysis, Investigation, Writing - original draft. **Steven Zhang:** Methodology, Writing - review & editing. **Lei Zhang:** Software. **Longfei Wang:** Investigation. **Hao Xue:** Software. **Zhong Lin Wang:** Supervision.

## Acknowledgements

## Appendix A. Supplementary data

Supplementary data to this article can be found online at https://doi.org/10.1016/j.nanoen.2020.104703.

## References

[1] Y.C. Lai, J. Deng, S.L. Zhang, S. Niu, H. Guo, Z.L. Wang, Single-thread-based wearable and highly stretchable triboelectric nanogenerators and their applications in cloth-based self-powered human-interactive and biomedical sensing, Adv. Funct. Mater. 27 (2016), 1604462, https://doi.org/10.1002/adfm.201604462.

[2] X. He, Y. Zi, H. Yu, S.L. Zhang, J. Wang, W. Ding, H. Zou, W. Zhang, C. Lu, Z. L. Wang, An ultrathin paper-based self-powered system for portable electronics and wireless human-machine interaction, Nano Energy 39 (2017) 328–336, https://doi.org/10.1016/j.nanoen.2017.06.046.

[3] S.L. Zhang, Y.C. Lai, X. He, R. Liu, Y. Zi, Z.L. Wang, Auxetic foam-based contact-mode triboelectric nanogenerator with highly sensitive self-powered strain sensing capabilities to monitor human body movement, Adv. Funct. Mater. 27 (2017), 1606695, https://doi.org/10.1002/adfm.201606695.

[4] M. Xu, P. Wang, Y.C. Wang, S.L. Zhang, A.C. Wang, C. Zhang, Z. Wang, X. Pan, Z. L. Wang, A soft and robust spring based triboelectric nanogenerator for harvesting arbitrary directional vibration energy and self-powered vibration sensing, Adv. Energy Mater. 8 (2017), 1702432, https://doi.org/10.1002/aenm.201702432.

[5] C. Qian, L. Li, M. Gao, H. Yang, Z. Cai, B. Chen, Z. Xiang, Z. Zhang, Y. Song, All-printed 3D hierarchically structured cellulose aerogel based triboelectric nanogenerator for multi-functional sensors, Nano Energy 63 (2019), 103885, https://doi.org/10.1016/j.nanoen.2019.103885.

[6] Q. Tang, X. Pu, Q. Zeng, H. Yang, J. Li, Y. Wu, H. Guo, Z. Huang, C. Hu, A strategy to promote efficiency and durability for sliding energy harvesting by designing alternating magnetic stripe arrays in triboelectric nanogenerator, Nano Energy 66 (2019), 104087, https://doi.org/10.1016/j.nanoen.2019.104087.

[7] S. Parandeh, M. Kharaziha, F. Karimzadeh, An eco-friendly triboelectric hybrid nanogenerators based on graphene oxide incorporated polycaprolactone fibers and cellulose paper, Nano Energy 59 (2019) 412–421, https://doi.org/10.1016/j.nanoen.2019.02.058.

[8] R.D.I.G. Dharmasena, S.R.P. Silva, Towards optimized triboelectric nanogenerators, Nano Energy 62 (2019) 530–549, https://doi.org/10.1016/j.nanoen.2019.05.057.

[9] J. Tao, R. Bao, X. Wang, Y. Peng, J. Li, S. Fu, C. Pan, Z.L. Wang, Self-powered tactile sensor array systems based on the triboelectric effect, Adv. Funct. Mater. 29 (2019) 1806379, https://doi.org/10.1002/adfm.201806379.

[10] J. Chen, H. Guo, Z. Wu, G. Xu, Y. Zi, C. Hu, Z.L. Wang, Actuation and sensor integrated self-powered cantilever system based on TENG technology, Nano Energy 64 (2019), 103920, https://doi.org/10.1016/j.nanoen.2019.103920.

[11] X. Meng, Q. Cheng, X. Jiang, Z. Fang, X. Chen, S. Li, C. Li, C. Sun, W. Wang, Z. L. Wang, Triboelectric nanogenerator as a highly sensitive self-powered sensor for driver behavior monitoring, Nano Energy 51 (2018) 721–727, https://doi.org/10.1016/j.nanoen.2018.07.026.

[12] X. Pu, H. Guo, Q. Tang, J. Chen, L. Feng, G. Liu, X. Wang, Y. Xi, C. Hu, Z.L. Wang, Rotation sensing and gesture control of a robot joint via triboelectric quantization sensor, Nano Energy 54 (2018) 453–460, https://doi.org/10.1016/j.nanoen.2018.10.044.

[13] C. Zhang, S. Liu, X. Huang, W. Guo, Y. Li, H. Wu, A stretchable dual-mode sensor array for multifunctional robotic electronic skin, Nano Energy 62 (2019) 164–170, https://doi.org/10.1016/j.nanoen.2019.05.046.

[14] Y. Chen, X. Pu, M. Liu, S. Kuang, P. Zhang, Q. Hua, Z. Cong, W. Guo, W. Hu, Z. L. Wang, Shape-adaptive, self-healable triboelectric nanogenerator with enhanced performances by soft solid–solid contact electrification, ACS Nano 13 (2019) 8936–8945, https://doi.org/10.1021/acsnano.9b02690.

[15] M. Xu, S. Wang, S.L. Zhang, W. Ding, P.T. Kien, C. Wang, Z. Li, X. Pan, Z.L. Wang, A highly-sensitive wave sensor based on liquid-solid interfacing triboelectric nanogenerator for smart marine equipment, Nano Energy 57 (2019) 574–580, https://doi.org/10.1016/j.nanoen.2019.05.046.

[16] X. Zhang, Y. Zheng, D. Wang, F. Zhou, Solid-liquid triboelectrification in smart U-tube for multifunctional sensors, Nano Energy 40 (2017) 95–106, https://doi.org/10.1016/j.nanoen.2017.08.010.

[17] B. Zhang, L. Zhang, W. Deng, L. Jin, F. Chun, H. Pan, B. Gu, H. Zhang, Z. Lv, W. Yang, Z.L. Wang, Self-powered acceleration sensor based on liquid metal triboelectric nanogenerator for vibration monitoring, ACS Nano 11 (2017) 7440–7446, https://doi.org/10.1021/acsnano.7b03818.

[18] X. Zhang, Y. Zheng, D. Wang, Z. UrRahmana, F. Zhou, Liquid–solid contact triboelectrification and its use in self-powered nanosensor for detecting organics in water, Nano Energy 30 (2016) 321–329, https://doi.org/10.1016/j.nanoen.2016.10.025.

[19] X. Zhang, M. Yu, Z. Ma, H. Ouyang, Y. Zou, S.L. Zhang, H. Niu, X. Pan, M. Xu, Z. Li, Z.L. Wang, Self-powered distributed water level sensors based on liquid–solid triboelectric nanogenerators for ship draft detecting, Adv. Funct. Mater. 29 (2019), 1900327, https://doi.org/10.1002/adfm.201900327.

[20] K.R. Wijewardhana, T.Z. Shen, E.N. Jayaweera, A. Shahzad, J.K. Song, Hybrid nanogenerator and enhancement of water–solid contact electrification using triboelectric charge supplier, Nano Energy 52 (2018) 402–407, https://doi.org/10.1016/j.nanoen.2018.08.016.

[21] H.C. Flemming, Biofouling in water systems–cases, causes and countermeasures, Appl. Microbiol. Biotechnol. 59 (2002) 629–640, https://doi.org/10.1007/s00253-002-1066-9.

[22] T. Artham, M. Sudhakar, R. Venkatesan, C.M. Nair, K.V.G.K. Murty, M. Doble, Biofouling and stability of synthetic polymers in sea water, Int. Biodeterior. Biodegrad. 63 (2009) 884–890, https://doi.org/10.1016/j.ibiod.2009.03.003.

[23] L.B. Huang, G. Bai, M.C. Wong, Z. Yang, W. Xu, J. Hao, Magnetic-assisted noncontact triboelectric nanogenerator converting mechanical energy into electricity and light emissions, Adv. Mater. 28 (2016) 2744–2751, https://doi.org/10.1002/adma.201505839.

[24] L.B. Huang, W. Xu, G. Bai, M.C. Wong, Z. Yang, J. Hao, Wind energy and blue energy harvesting based on magnetic-assisted noncontact triboelectric nanogenerator, Nano Energy 30 (2016) 36–42, https://doi.org/10.1016/j.nanoen.2016.09.032.

[25] L.B. Huang, W. Xu, W. Tian, J.C. Han, C.H. Zhao, H.L. Wu, J. Hao, Ultrasonic-assisted ultrafast fabrication of polymer nanowires for high performance triboelectric nanogenerators, Nano Energy 71 (2020), 104593, https://doi.org/10.1016/j.nanoen.2020.104593.

[26] A. Ray, V.B. Varma, P.J. Jayaneel, N.M. Sudharsan, Z.P. Wang, R.V. Ramanujan, On demand manipulation of ferrofluid droplets by magnetic fields, Sensor. Actuator. B Chem. 39 (2017) 328–336, https://doi.org/10.1016/j.snb.2016.11.115.

[27] C. Rigoni, S. Bertoldo, M. Pierno, D. Talbot, A. Abou-Hassan, G. Mistura, Division of ferrofluid drops induced by a magnetic field, Lanmuir 34 (2018) 9762–9767, https://doi.org/10.1021/acs.langmuir.8b02399.

[28] E. Rodríguez-Schwendtner, N. Díaz-Herrera, M.C. Navarrete, A. González-Cano, Ó. Esteban, Plasmonic sensor based on tapered optical fibers and magnetic fluids for measuring magnetic fields, Sensor Actuat. A-Phys. 264 (2017) 58–62, https://doi.org/10.1016/j.sna.2017.07.040.

[29] J. Nie, Z. Wang, Z. Ren, S. Li, X. Chen, Z.L. Wang, Power generation from the interaction of a liquid droplet and a liquid membrane, Nat. Commun. 10 (2019) 2264, https://doi.org/10.1038/s41467-019-10232-x.

[30] P. Jiang, L. Zhang, H. Guo, C. Chen, C. Wu, S. Zhang, Z.L. Wang, Signal output of triboelectric nanogenerator at oil–water–solid multiphase interfaces and its application for dual-signal chemical sensing, Adv. Mater. 31 (2019), 1902793, https://doi.org/10.1002/adma.201902793.

[31] J. Li, E. Ueda, D. Paulssen, P.A. Levkin, Slippery lubricant-infused surfaces: properties and emerging applications, Adv. Funct. Mater. 29 (2019), 1802317, https://doi.org/10.1002/adfm.201802317.

[32] G.H. Zhu, S.H. Cho, H. Zhang, M. Zhao, N.S. Zacharia, Slippery liquid-infused porous surfaces (SLIPS) using layer-by-layer polyelectrolyte assembly in organic solvent, Langmuir 34 (2018) 4722–4731, https://doi.org/10.1021/acs.langmuir.8b00335.

[33] T.S. Wong, S.H. Kang, S.K.Y. Tang, E.J. Smythe, B.D. Hatton, A. Grinthal, J. Aizenberg, Bioinspired self-repairing slippery surfaces with pressure-stable omniphobicity, Nature 477 (2011) 443–447, https://doi.org/10.1038/nature10447.

**Peng Wang** received his B.S. (2003) in Chemical Engineering & Technology, and Ph.D. (2009) in Chemical Engineering from Dalian University of Technology. Currently, he is working as a full professor in Institute of Oceanology, Chinese Academy of Sciences. His research interests include triboelectric nanogenerators, corrosion protection, anti-biofouling technology.

**Steven Zhang** received his B.S. degree in Electronic Materials Engineering from U.C. Davis in 2014. He is currently pursuing a Ph.D. in Material Science and Engineering at Georgia Institute of Technology, and is working for Professor Zhong Lin Wang. His research focuses on nanogenerators, energy harvesting, and self-powered active sensing.

**Hao Xue** received his B.S. (2001) in Materials Science and Engineering and Ph.D. (2006) in Materials Science and Engineering from Tsinghua University. Currently, he is an associate professor at Department of Materials Science and Engineering, Xiamen University. His research interests include piezoelectric materials and devices, triboelectric nanogenerators.

**Dr. Lei Zhang** received his Ph.D. in Materials Science and Engineering from Southwest Jiaotong University, Chengdu in 2019. His current research interests include energy harvesting triboelectric nanogenerators, and flexible self-powered sensors.

**Zhong Lin (ZL) Wang** received his Ph.D. from Arizona State University in physics. He now is the Hightower Chair in Materials Science and Engineering, Regents' Professor, Engineering Distinguished Professor and Director, Center for Nanostructure Characterization, at Georgia Tech. Dr. Wang has made original and innovative contributions to the synthesis, discovery, characterization and understanding of fundamental physical properties of oxide nanobelts and nanowires, as well as applications of nanowires in energy sciences, electronics, optoelectronics and biological science. His discovery and breakthroughs in developing nanogenerators established the principle and technological road map for harvesting mechanical energy from environment and biological systems for powering a personal electronics. His research on self-powered nanosystems has inspired the worldwide effort in academia and industry for studying energy for micro-nano-systems, which is now a distinct disciplinary in energy research and future sensor networks. He coined and pioneered the field of piezotronics and piezophototronics by introducing piezoelectric potential gated charge transport process in fabricating new electronic and optoelectronic devices. Details can be found at: http ://www.nanoscience.gatech.edu.

**Longfei Wang** received his B.S. (2012) in Materials Science and Engineering from China University of Geosciences (Beijing) and Ph.D. (2017) in Nanoscience and Technology from Beijing Institute of Nanoenergy and Nanosystems, Chinese Academy of Sciences. He is now a postdoctoral fellow in Professor Zhong Lin Wang's group at Georgia Institute of Technology. His current research focuses on piezotronics and piezophototronics.